ORIGINAL ARTICLE

The effect of maternal type 2 diabetes on fetal endothelial gene expression and function

Samar Sultan[1] ®

Abstract

Aims Maternal type 2 diabetes (T2D) can result in adverse pathological outcomes to both the mother and fetus. The present study aimed to investigate the pathological effects of maternal T2D on the gene expression patterns and functions of fetal human umbilical vein endothelial cells (HUVECs), a representative of fetal vascular cells.

Methods Cell proliferation, apoptosis, mitochondrial ROS production and cell cycle were measured using flowcytometry. Genome-wide expression was measured using Affymetrix microarray. Gene expression of *CCND2, STAT1, ITGB8, ALDH2, and ADAMTS5* was measured using real-time PCR.

Results HUVECs derived from T2D mothers (T2D-HUVECs) showed elevated levels of mitochondrial superoxide anions, reduced cell proliferation, and increased apoptosis rates relative to HUVECs derived from healthy control mothers (C.HUVECs). In addition , T2D-HUVECs showed a decreased proportion of cells in G0/G1 and cell cycle arrest at the S phases relative to controls. Interestingly, microarray experiments revealed significant differences in genome-wide expression profiles between T2D-HUVECs and C.HUVECs. In particular, the analysis identified 90 upregulated genes and 42 downregulated genes. The upregulated genes *CCND2, STAT1, ITGB8, ALDH2*, and *ADAMTS5* were validated as potential biomarkers for fetal endothelial dysfunction. Functional network analysis revealed that these genes are the important players that participate in the pathogenesis of endothelial dysfunction, which in turn influences the inflammatory response, cellular movement, and cardiovascular system development and function.

Conclusion Sustained alterations in the overall function of T2D-HUVEC and gene expression profiles provided insights into the role of maternal T2D on the pathophysiology of the fetal endothelial dysfunction.

Keywords Type 2 diabetes · Endothelial cells · Oxidative stress · Genome-wide gene expression · Dysfunction

Abbreviations

MMPs	ADAMTS are zinc metalloproteases	C.HUVEC	Healthy control cells
AGE	Advanced glycation end products	T2D-HUVECs	HUVECs derived from T2D mothers
ECs	Endothelial cells	T2D	Type 2 diabetes
ET-1	Endothelin 1	NO	Nitric oxide
ECM	Extracellular matrix	PKC	Protein kinase C
GDM	Gestational diabetes mellitus	PI	Propidium iodide
		ROS	Reactive oxygen species

✉ Samar Sultan
sasultan@kau.edu.sa

1 Medical Technology Department, Faculty of Applied Medical Sciences, King Abdulaziz University, Jeddah, Saudi Arabia

Introduction

Diabetes is a complex disease characterized by hyperglycemia, which is a key player in the initiation of diabetes complications, such as cardiovascular diseases. Given the increasing rates of diabetes worldwide, more studies are required to elucidate the mechanisms underlying the pathogenesis of diabetes. The endothelium plays critical roles in the regulation of vascular tone, angiogenesis, inflammatory

responses, coagulation, and fibrinolysis [1]. The dysfunctional endothelium is known to exhibit changes in the functions of normal endothelial cells (ECs) and is characterized by decreased nitric oxide (NO)-induced vasodilation, increased expression of inflammatory adhesion molecules, increased endothelin 1 (ET-1)-induced vasoconstriction, and impaired balance between coagulation and fibrinolysis, which in turn promotes platelet activation and thrombus formation [2].

Various factors, including hyperglycemia-induced oxidative stress, contribute to endothelial dysfunction in diabetes. Hyperglycemia has been demonstrated to cause oxidative stress via the overproduction of free radicals or impairment of the antioxidant defense [3]. A previous study showed that fetal HUVECs exposed to maternal diabetes (GDM) showed enhanced oxidative stress [4]. Hyperglycemia is thought to stimulate various cellular processes, such as glucose autoxidation, production of advanced glycation end products (AGE), and protein kinase C (PKC) activation [5, 6]. These events lead to excessive production of reactive oxygen species (ROS) and increased oxidative stress, which in turn impair the antioxidant defense system. Previous studies have shown that fetal cord blood from GDM mothers exhibited downregulation of antioxidant enzymes and upregulation of oxidative stress markers, such as xanthine oxidase, a major superoxide-producing enzyme [7].

In addition, hyperglycemia is known to delay cell proliferation and promote apoptosis in human vascular ECs and is known to contribute to diabetic complications [8, 9]. In vitro experiments on HUVECs derived from GDM patients and ECs exposed to elevated glucose levels have reported similar effects on cell proliferation [4, 10]. However, cell proliferation and apoptosis rates in HUVECs derived from T2D mothers under normoglycemic conditions have not been previously reported.

Early studies by Barker et al. suggested that most diseases can be programmed during in utero fetal development [11]. Moreover, an increasing body of evidence has shown that fetal exposure to maternal diabetes in utero increases the susceptibility of offspring to develop diseases, such as diabetes, later in life through a mechanism independent from genetic transmission. One study reported that offspring exposed to maternal T2D during pregnancy exhibited a higher risk of developing T2D (45%) than the offspring of non-diabetic mothers (1.4%) or pre-diabetic mothers (8.6%) [12]. Consistent with the above findings, Dabelea et al. showed that offspring prenatally exposed to T2D exhibited higher prevalence of T2D, with the T2D rate peaking at 70% in individuals aged 23–34 years old. On the other hand, the offspring of non-diabetic mothers showed lower than the 15% rate of developing diabetes within a similar age range [13]. Accordingly, these epidemiological studies suggested that intrauterine exposure to diabetes is responsible for "programming" abnormal glucose homeostasis (glycemic or metabolic memory) in offspring in addition to the effects conferred by genetic factors. However, the molecular basis underlying fetal programming remains unclear. Therefore, we aimed to investigate the mechanisms underlying fetal endothelial dysfunction and to compare the effects of in utero exposure to maternal T2D on cell proliferation, apoptosis, cell cycle, mitochondrial superoxide, and genome-wide gene expression profiles of ECs cultured under physiological glucose conditions (5 mM) relative to healthy control cells (C.HUVECs).

Materials and methods

All materials were purchased from Sigma (Poole, UK) unless otherwise stated.

Study subjects

Umbilical cords were collected from a total of 17 T2D mothers and seven healthy mothers immediately after full-term delivery in the Obstetrics and Gynecology Department of the King Abdulaziz University Hospital, Jeddah, Saudi Arabia. All donors were informed about the objectives of the research, and informed consent was obtained from each study participant prior to sample collection. This study was approved by the Ethics Committee of the King Abdulaziz University Hospital. The selection of control subjects was from among pregnant women with normal plasma glucose (fasting or random). Exclusion criteria for the control group were as follows: donors on medication or who have a family history of diabetes and/or high blood pressure and/or are smokers. The selection of diabetic subjects was from among pregnant women with a plasma glucose concentration (fasting or random) > 7 mmol/L or HbA1c > 7% according to the American Diabetes Association [14]. Notably, patients participating in this study had no other obstetric complications. All T2D patients were on insulin along with other medications, such as metformin and novorapid. Basic anthropometric parameters, including height, weight, and body mass indices, were recorded at approximately 12 weeks of pregnancy.

Isolation and culture of HUVECs

ECs were harvested from freshly collected HUVECs following normal delivery from T2D mothers (experimental groups) and healthy mothers (control groups). Collected cords were stored at 4 °C in RPMI-1640 media containing heparin (10 U/mL), fungizone (2.5 µg/mL), penicillin, and streptomycin (100 U/100 mg/mL) until subsequent processing. ECs were isolated from the human umbilical vein by

treatment with collagenase enzyme as described in Eccles [15]. Afterwards, HUVECs were grown to confluence in complete culture medium M199 containing 5 mM glucose, 20% fetal bovine serum, penicillin/streptomycin (100 U/100 mg/mL), fungizone (2.5 µg/mL), and L-glutamine (2 mM) at 37 °C under 95% air and 5% CO_2 humidified conditions. ECs were used for up to four passages. For all experiments, at least three subjects were analyzed from each group.

Cell proliferation

For flow cytometry, ECs were labeled using a CellTrace™ Violet Cell Proliferation Kit (Invitrogen, Carlsbad, CA, USA) according to the manufacturer's instructions. Briefly, ECs were washed with 1× PBS and re-suspended in 1 µM working dye solution in 1× PBS for 20 min at 37 °C. Then, the cell mixtures were added with five volumes of cell culture medium and incubated at room temperature for 5 min to remove free dyes. Afterwards, labeled ECs were centrifuged and re-suspended in culture medium and incubated for 48 h. Labeled ECs were then harvested and analyzed on a FACS Aria III flow cytometer (BD Biosciences, San Jose, USA), capturing at least > 20,000 events per run.

Apoptosis assay

Flow cytometry was performed using Dead Cell Apoptosis Kit with Annexin V FITC and PI (Invitrogen, Carlsbad, CA, USA) following the manufacturer's instructions. Briefly, ECs were washed twice with cold PBS, suspended in 250 µL of annexin V binding buffer, and subsequently incubated with 2.5 µL of annexin V and 2.5 µL of PI for 5 min at room temperature in the dark. Non-stained cells were used as negative controls. Labeled cells were immediately analyzed by acquiring 10,000 cellular events on a FACS Aria III flow cytometer (BD Biosciences, San Jose, USA) using 88-nm excitation and a 525-nm band pass filter for FITC and a 620-nm filter for PI detection.

Mitochondrial ROS production (mtROS) determination

Reactive oxygen species (ROS) levels released from mitochondria were determined using MitoSOX™ Red reagent (Invitrogen, Carlsbad, CA, USA) according to the protocol as described previously [16]. The MitoSOX™ Red dye is rapidly oxidized by mitochondrial superoxide but not by other ROS and reactive nitrogen species (RNS). Briefly, ECs were incubated in Hank's buffer containing 2 µM MitoSOX Red for 30 min at 37 °C and under 5% CO_2 conditions. Non-stained cells served as negative control. After incubation, ECs were washed with PBS, and fluorescence intensities were assessed using a FACS Aria III flow cytometer (BD Biosciences, San Jose, USA).

Cell cycle analysis

For cell cycle analysis, the DNA contents of cell nuclei were determined via propidium iodide (PI) staining, in which the signals obtained from PI are proportional to the amount of DNA present in the cells [17]. ECs were harvested by trypsin treatment and stained with FxCycle™ PI/RNase Staining Solution (Molecular Probes, Life Technologies) according to the manufacturer's instructions. Samples were analyzed using a FACS Aria III flow cytometer (BD Biosciences, San Jose, USA); at least 35,000 events were captured per analysis. Cell cycle analysis was performed using Flowlogic™ Software (version 7.2).

RNA isolation

Total RNA was isolated from HUVECs using the RNeasy mini kit (Qiagen, Crawley, UK). RNA concentration and purity were assessed spectrophotometrically. RNA integrity was evaluated using an Agilent 2100 Bioanalyzer (Agilent, Edinburgh, UK). RNA samples were stored at −80 °C until further microarray analysis.

Real-time PCR

cDNA was synthesized from 1 µg of RNA using an ImProm-II Reverse Transcription System kit (Promega, Southampton, UK) following the manufacturer's protocols. Primers were designed using the Primer3Primer software. All primer sequences are summarized in Supplementary Table 1 (Online Resource 1). β-Actin was used as an internal control for normalization of the mRNA levels. Amplifications were performed in duplicates using a QuantiTect SYBR Green PCR kit (Qiagen, Manchester, UK) on an iCycleriQ Real-time PCR Detection System (Applied Biosystem, Cheshire, UK), according to the manufacturer's instructions. Reactions were run according to the following profile: 10 min denaturing at 95 °C; and 40 cycles of denaturing 95 °C for 15 s, annealing at 63 °C for 10 s, and extension 72 °C for 20 s. Relative expression levels were determined using Rest 2009 software version 2.0.13 [18].

Microarray processing

GeneChip™ Whole Transcript PLUS kit (Affymetrix, USA) was used to generate and amplify fluorescent cRNA from total RNA (250 ng/sample). The generated cRNAs were then hybridized to Human Gene 2.0 ST arrays (Affymetrix, USA), which measures the signals for > 30,000 coding transcripts and > 11,000 long intergenic non-coding transcripts.

The Affymetrix GeneChip Hybridization, Wash and Stain Kit was used for hybridization. Sample hybridization to microarray GeneChip and image scanning was performed according to the manufacturers' instructions.

Microarray analysis

Microarray expression data were imported into Partek Genomics Suite version 6.6 (Partek Inc., MO, USA). Data were normalized to minimize the effects of systematic non-biological variations. The analysis was focused on the genes with a fold change ≥ 1.5 and p value < 0.05 in T2D-HUVECs relative to C.HUVECs.

The Partek Gene Ontology (GO) enhancement tool was utilized in the gene expression analysis to classify the differentially expressed genes (T2D-HUVECs and C.HUVECs) according to the cellular component, molecular function, and biological process categories [19].

The Ingenuity Pathways Analysis programming (IPA) (Ingenuity Systems, Redwood City, CA, USA) was also utilized to further analyze the gene expression data. IPA results were ranked based on statistical scores. The IPA workflow included core and functional analysis and structural categorization. Canonical pathway investigation incorporated overlay analysis of predefined pathways using the gene list as input.

Statistical analysis

Unpaired data were analyzed using Student's t-test. Results are presented as mean $\pm$ SEM. Statistically significant differences were considered at $p < 0.05$.

Results

Clinical characteristics of the subjects recruited in the present study are summarized in Table 1. HbA1c and random plasma glucose levels were significantly higher in T2D women than those in the healthy controls. The T2D group showed a near-significant increase in FPG levels relative to those in the control group. In addition, there were no significant differences in age and BMI between the two groups.

Effects of T2D on proliferation, apoptosis and superoxide production in HUVECs.

As shown in Fig. 1a, b, T2D significantly reduced ($p = 0.006$, $n = 4$–5) the proliferation rates of HUVECS relative to C.HUVECs. Furthermore, apoptosis rates were significantly higher ($p = 0.04$, $n = 4$) in T2D-HUVECs than in C.HUVECs (Fig. 1c, d). Interestingly, superoxide production in the mitochondria of T2D-HUVECs was significantly higher ($p = 0.0002$, $n = 4$–6) than those in the controls (Fig. 2).

Effect of T2D on the cell cycle

Propidium iodide (PI) staining and flow cytometry analysis revealed that T2D significantly reduced the proportion of HUVECs in the G0/G1 phase of the cell cycle ($p = 0.008$, $n = 4$–5). Moreover, T2D induced a greater proportion of cells in cell cycle arrest in the S phase ($p = 0.047$, $n = 4$–5) in HUVECs than in C.HUVECs (Fig. 3).

Differential gene expression analysis of T2D-HUVEC and C.HUVECs.

Our analysis identified a total of 132 differentially expressed transcripts between T2D-HUVECs and C.HUVECs (FDR-adjusted p value < 0.05 and fold change > 1.5). In particular, a total of 90 genes were upregulated and 42 genes were downregulated in T2D-HUVECs relative to C.HUVECs. The most significantly upregulated genes in T2D-HUVEC included *ITGB8, CCND2, ALDH2, STAT1*, and *ADAMTS5* (Table 2). Hierarchical cluster analysis determines groups of genes that 132 differentially expressed genes between C.HUVECs and T2D-HUVEC (Fig. 4a).

Network and pathway analysis

A functional annotation network was generated using IPA based on the network relationships determined in

Table 1 Mean characteristics of subjects participating in the study

Status mothers	Controls ($n = 7$)	T2D ($n = 17$)	p (T2D versus controls)
Age (years)	29 ± 0.3	33 ± 0.2	0.06
BMI	28.8 ± 0.5	33.1 ± 0.3	0.09
HbA1c % (mmol/mol)	$5 (31) \pm 0.02$ ($n = 3$)	$8 (64) \pm 0.2$ ($n = 16$)	0.005
RPG (mM)	4.6 ± 0.04	8.1 ± 0.2	0.002
FPG (mM)	5.1 ± 0.1 ($n = 4$)	7.5 ± 0.3 ($n = 9$)	0.05

Number of donors donated by (n)

RPG, Random plasma glucose; FPG, fasting plasma glucose; BMI, body mass index, HbA1c, glycosylated hemoglobin; T2D, type 2 diabetes mellitus, mean $\pm$ SEM

Fig. 1 HUVEC cell proliferation and apoptosis. **a** A representative image of the proliferation flowcytometry. C.HUVEC and T2D-HUVEC were labeled with 1 μM CellTrace violet and culture for 2 days, after that the cell proliferation was determined by flowcytometry. **b** Percentage cell proliferation for both C.HUVEC ($n = 4$) and T2D-HUVEC ($n = 5$). **c** A representative image of the apoptosis flowcytometry. Harvested Cells after 2-day culture were labeled with Annexin-V FTTC-A dye and the cell apoptosis were determined by flowcytometry. **d** Percentage apoptosis for both C.HUVEC ($n = 4$) and T2D-HUVEC ($n = 5$). Data are presented as means ± SEM. *$p < 0.05$ versus controls
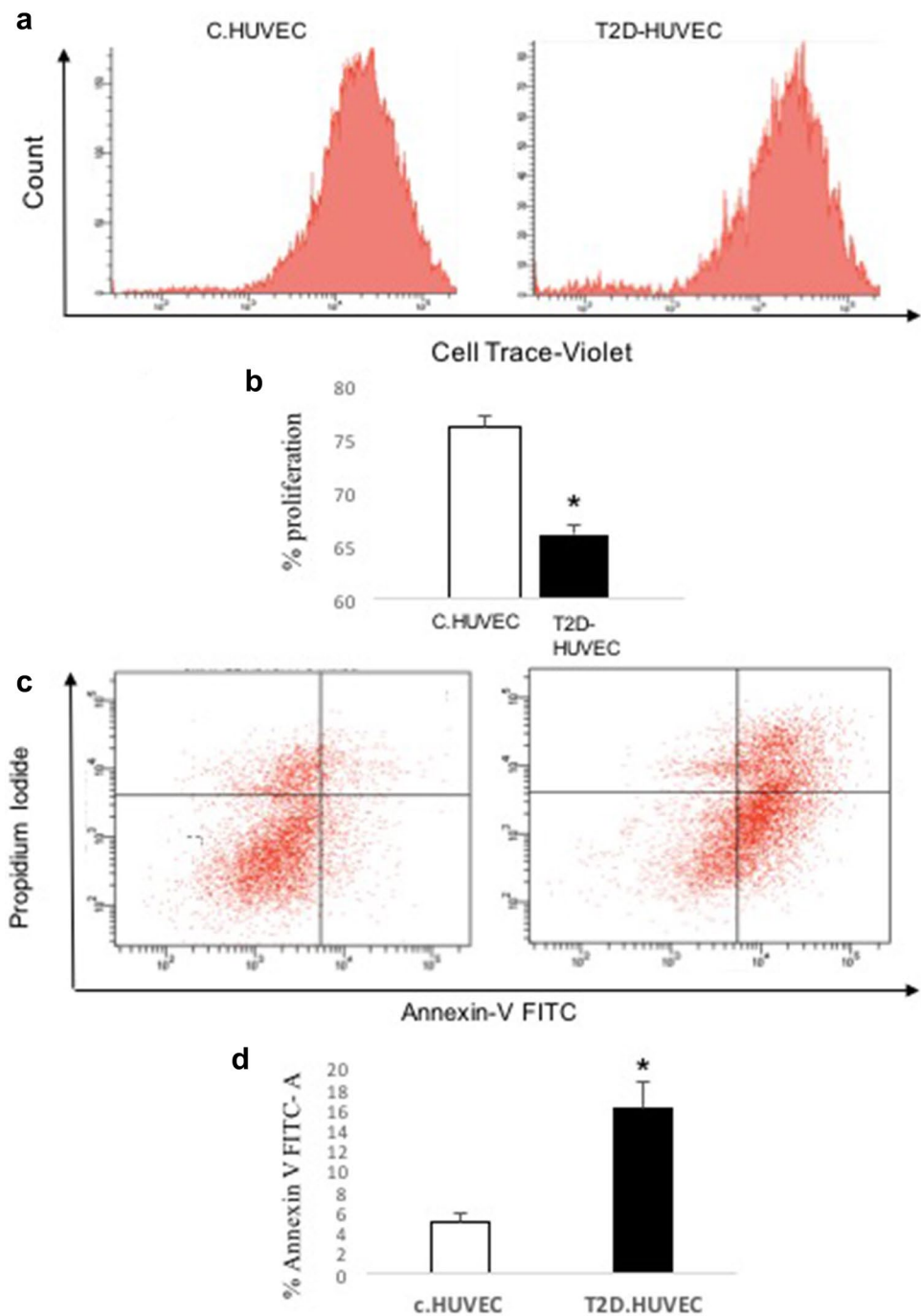

the 132 differentially expressed genes. Network analysis showed that these genes were involved in inflammatory response, cellular movement, cell signaling, organ development, DNA damage and repair, and cardiovascular system development and function (Supplementary Table 2, Online Resource 1). Interferon signaling was identified as the most significant canonical pathway associated with the differentially expressed gene set ($p = 1.57 \times 10^{-2}$; data not shown).

Validation with real-time PCR

The present analysis focused on the genes involved in inflammatory response, cell movement and cardiovascular system development and function since these are the most likely to be of relevance to the pathogenesis of diabetes cardiovascular complications (Supplementary Table 2, Online Resource 1). Combining the list of upregulated genes (Table 2) and genes clusters in Supplementary Table 2 (Online Resource

Fig. 2 HUVEC mitochondrial superoxide production. **a** A representative image of the mitochondrial superoxide flow-cytometry. Cells were labeled with MitoSOX Red mitochondrial superoxide indicator staining and the cells superoxide was determined by flowcytometry. **b** Percentage of superoxide production in both C.HUVEC ($n=4$) and T2D-HUVEC ($n=6$). Data are presented as means $\pm$ SEM. $**p < 0.001$ versus controls
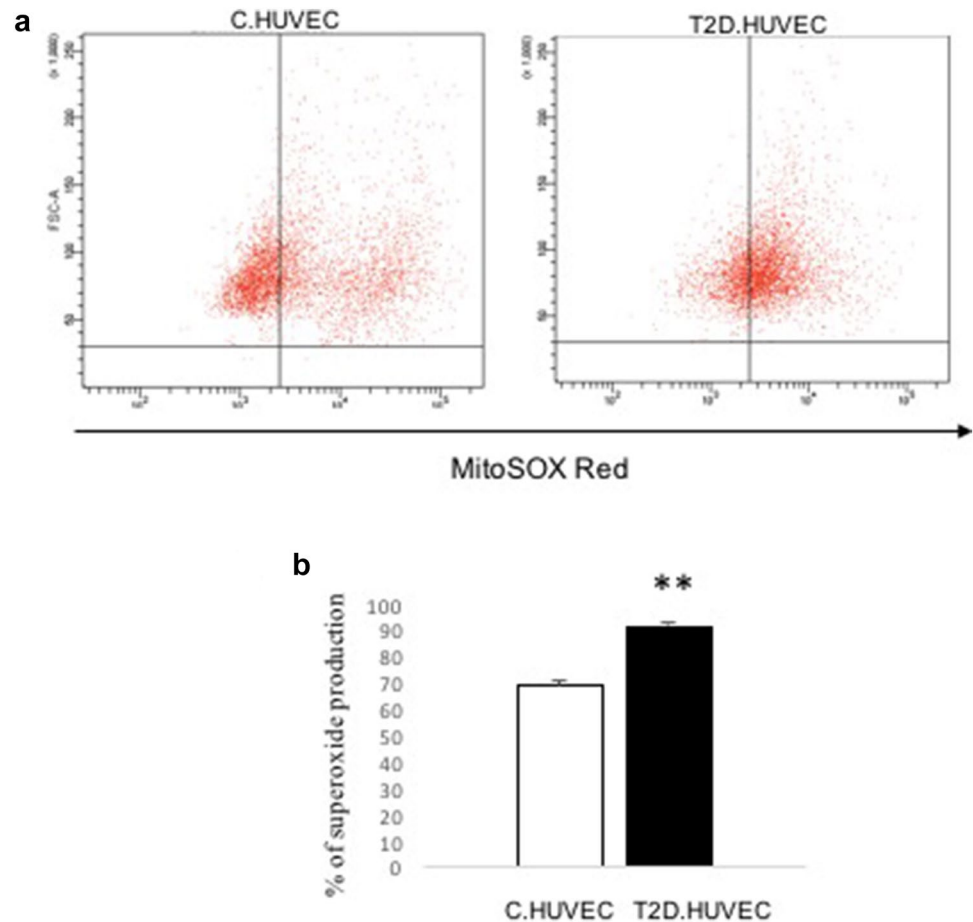
1), we selected five genes (ITGB8, STAT1, CCND2, ALDH2, and ADAMTS5) for further validation. Real-time PCR validation showed that these five gene transcripts were significantly altered ($p < 0.05$), with a fold change ≥ 1.5 (Table 2 and Supplementary Table 2, Online Resource 1). The mRNA levels were consistent with those obtained in the microarray experiment. ITGB8, STAT1, CCND2, ALDH2, and ADAMTS5 around 3.4- ($p = 0.0001$, $n = 3$), 3.6- ($p = 0.0001$, $n = 3$), 2.1- ($p = 0.034$, $n = 3$), 2.5- ($p = 0.034$, $n = 3$), and 5-fold ($p = 0.0001$, $n = 3$) upregulated, respectively, in T2D-HUVECs relative to C.HUVECs (Fig. 4b).

Discussion

Our current findings suggested that maternal T2D induced mitochondrial oxidative stress, inhibited cell proliferation, increased apoptosis, and altered the cell cycle distribution in fetal HUVECs. Moreover, our microarray results identified 132 differentially expressed transcripts in HUVECs derived from T2D mothers when compared to C.HUVECs. Taken together, our findings indicated that T2D-HUVECs exhibited persistent dysfunctional characteristics even after subsequent culture under normoglycemic conditions, thereby providing evidence of metabolic memory.

Oxidative stress caused by increased mitochondrial superoxide production has been implicated in the development of the dysfunctional endothelium [20]. Our current findings showed that T2D-HUVECs generated excessive amounts of superoxide in the mitochondria when compared to C.HUVECs. Thus, exposure to elevated glucose levels in the womb contributes to a sustained increased in oxidative stress under normoglycemic conditions. Consistent with the above-mentioned findings, hyperglycemia was found to induce changes in the expression of genes involved in oxidative stress in HUVECs [21]. Interestingly, oxidative stress has been reported to be involved in metabolic memory through epigenetic mechanisms that induce persistent changes in gene expression even after glucose normalization in HUVECs [22].

In the present study, our results showed that cell proliferation rates were significantly lower in T2D-HUVECs than in C.HUVECs when cultured at 5 mM glucose for 48 h. This is consistent with a previous study that demonstrated reduced cell growth in the dermal microvascular endothelial cell exposed to elevated glucose levels (30 mM) for 7

Fig. 3 HUVEC distribution in cell cycle phases including G0/G1, S and G2/M phase. **a** A representative image of the cell cycle flowcytometry. Cells were fixed overnight with ethanol and labeled with FxCycle™ PI/RNase stain and the cell cycle distribution was determined by flowcytometry. **b** Percentage of both C.HUVEC ($n=4$) and T2D-HUVEC ($n=5$) distribution in each cell cycle phases. Data are presented as means ± SEM. *$p<0.05$, **$p<0.001$ versus controls
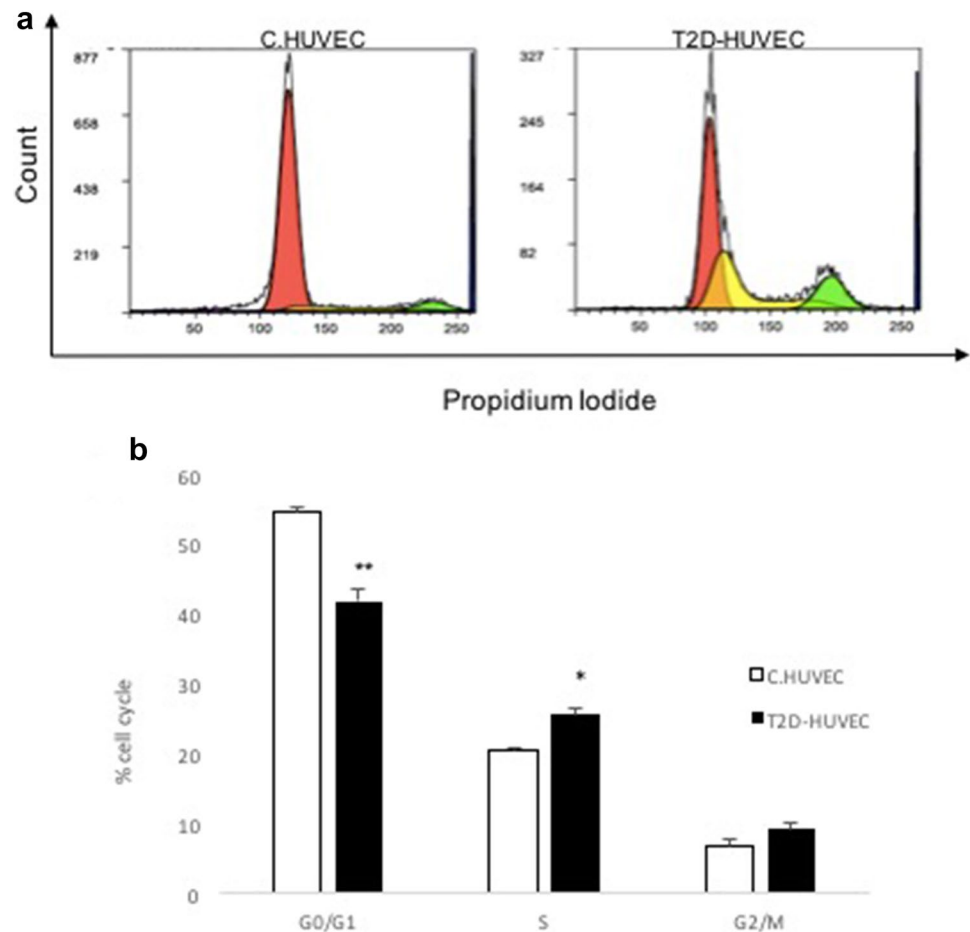
days relative to control cells cultured under normoglycemic conditions [9]. However, our findings were contradictory to the results of one study that reported no significant differences between the [³H] thymidine incorporation of HUVECs isolated from type 1 diabetic mothers and control HUVECs after 72 h of incubation in medium containing physiological 5 mM glucose [23]. This could be attributed to the fact that the ECs in the present study were isolated from different diabetic-type pregnancies from T2D mothers or could be explained by differences in the analytical methods used.

Apoptosis plays an important role in maintaining the homeostasis of different tissues in the adult human body. In the present study, T2D-HUVECs showed higher apoptosis rates relative to C.HUVECs, consistent with studies showing that HUVECs cultured under hyperglycemic conditions showed higher apoptosis rates than HUVECs cultured under normal glucose conditions [8]. Results showed increased apoptosis and reduced proliferation in T2D-HUVECs compared to C.HUVECs. Furthermore, loss of homeostasis may lead to vascular endothelial injury, which can trigger the pathogenesis of vascular disease complications, such as atherosclerosis. Endothelial cell dysfunction is widely believed to precede the development of atherosclerosis [24]. Thus, in

the present study, the increased apoptosis rates observed in T2D-HUVECs could be explained by increased oxidative stress, which is considered to initiate apoptosis by reducing the expression of XIAP, an anti-apoptotic protein, in other models [25].

The cell cycle consists of three phases, namely, the cell proliferation phase (G0/G1), DNA replication phase (S phase) and mitosis phase (G2/M phase) [26]. Hyperglycemia has been demonstrated to induce DNA damage and delay cell cycle progression in ECs [27, 28]. Our study is the first to demonstrate that T2D-HUVECs-induced cell cycle arrest in the S phase and inhibit the entry into the G0/G1 phase. Furthermore, our results indicated that maternal T2D triggers in utero programming of dysfunctional endothelium and can confer susceptibility to the development of vascular diseases in later life.

In addition, we conducted microarray experiments to compare the differences in gene expression profiles between T2D-HUVECs and C.HUVECs under normoglycemic conditions. We believe that such comparisons reflect the pathological changes in the metabolic and other cellular pathways in the ECs and allow us to establish the link between these molecular mechanisms and potential consequences in terms

Table 2 List of selected differentially upregulated and downregulated genes in T2D-HUVEC versus C.HUVEC

| Gene symbol	Fold change	p value	Gene name
LINC00440	13.2	0.035	Long intergenic non-protein-coding RNA 440
LOC105378325	7.20	0.007	Uncharacterized LOC105378325
BEX1	6.77	0.018	Brain-expressed X-linked 1
CD24	5.88	0.041	CD24 molecule
GJA5	5.53	0.008	Gap junction protein alpha 5
ITGB8	4.42	0.021	Integrin beta 8
CADM3	4.05	0.014	Cell adhesion molecule 3
GFRA1	3.59	0.008	GDNF family receptor alpha 1
LOC105377378	3.50	0.028	Uncharacterized LOC105377378
RFPL4AL1	3.40	0.022	Ret finger protein-like 4A-like 1
CYTL1	3.36	0.022	Cytokine-like 1
LOC105378477	3.12	0.045	Uncharacterized LOC105378477
LINC01040	2.81	0.015	Long intergenic non-protein-coding RNA 1040
CUBN	2.79	0.010	Cubilin (intrinsic factor–cobalamin receptor)
RELN	2.71	0.014	Reelin
KCNMB1	2.64	0.031	Potassium channel subfamily M regulatory beta subunit 1
MAP2	2.61	0.028	Microtubule-associated protein 2
CCND2	2.51	0.033	Cyclin D2
MYOZ2	2.46	0.005	Myozenin 2
OCIAD2	2.38	0.023	OCIA domain-containing 2
UPP1	2.36	0.006	Uridine phosphorylase 1
UNC13D	2.35	0.032	unc-13 homolog D (*C. elegans*)
DDX58	2.27	0.044	DEAD (Asp–Glu–Ala–Asp) box polypeptide 58
LOC440300	2.26	0.044	Chondroitin sulfate proteoglycan 4 pseudogene
PPP4R4	2.15	0.014	Phosphatase 4, regulatory subunit 4
GLB1L	2.15	0.005	Galactosidase beta 1 like
LOC105375721	2.11	0.010	Uncharacterized LOC105375721
PGM5P2	2.06	0.001	Phosphoglucomutase 5 pseudogene 2
ADAMTS5	2.03	0.042	ADAM metallopeptidase with thrombospondin
LOC100129434	1.97	0.023	Uncharacterized LOC100129434
PVR	1.95	0.047	Poliovirus receptor
KIF5A	1.94	0.008	Kinesin family member 5A
TNFRSF10A	1.92	0.021	Tumor necrosis factor receptor superfamily
LINC00571	1.90	0.014	Long intergenic non-protein-coding RNA 571
CD177	1.90	0.025	CD177 molecule
KIF1A	1.89	0.008	Kinesin family member 1A
ARMCX2	1.83	0.008	Armadillo repeat containing, X-linked 2
PIK3IP1	1.80	0.004	Phosphoinositide-3-kinase-interacting protein 1
SLC16A6	1.79	0.027	Solute carrier family 16, member 6
RND3	1.79	0.039	Rho family GTPase 3
SPRN	1.76	0.002	Shadow of prion protein homolog (zebrafish)
STAT1	1.75	0.029	Signal transducer and activator of transcription 1
PRKG1-AS1	1.74	0.008	PRKG1 antisense RNA 1
IDUA	1.74	0.009	Iduronidase, alpha-L
SLC43A2	1.74	0.048	Solute carrier family 43 (amino acid system L transporter)
B3GALT1	1.70	0.039	UDP-Gal:betaGlcNAc beta 1,3-galactosyltransferase 1
C11orf63	1.70	0.048	Chromosome 11 open reading frame 63
PGM2L1	1.70	0.042	Phosphoglucomutase 2-like 1
MIR4253	1.70	0.010	MicroRNA 4253
COL25A1	1.69	0.049	Collagen, type XXV, alpha 1

Table 2 (continued)

Gene symbol	Fold change	*p* value	Gene name
LINC01336	1.69	0.011	Long intergenic non-protein-coding RNA 1336
PSG9	1.68	0.028	Pregnancy-specific beta-1-glycoprotein 9
EFCAB13	1.67	0.010	EF-hand calcium-binding domain 13
RRAGB	1.67	0.019	Ras-related GTP-binding B
LOC105378596	1.65	0.003	Uncharacterized LOC105378596
TPPP	1.64	0.043	Tubulin polymerization-promoting protein
STK17A	1.64	0.040	Serine/threonine kinase 17a
ALDH2	1.62	0.013	Aldehyde dehydrogenase 2 family (mitochondrial)
RASA4B	− 1.52	0.047	RAS p21 protein activator 4B
TRABD2B	− 1.52	0.018	TraB domain-containing 2B
LINC01121	− 1.52	0.035	Long intergenic non-protein-coding RNA 1121
SLC8A1	− 1.53	0.045	Solute carrier family 8 (sodium/calcium exchanger), member 1
PHLDA3	− 1.56	0.038	Pleckstrin homology-like domain, family A, member 3
SPDYE18	− 1.56	0.038	Speedy/RINGO cell cycle regulator family member E18
CHEK2P2	− 1.59	0.015	Checkpoint kinase 2 pseudogene 2
FCHO1	− 1.59	0.006	FCH domain only 1
ARL10	− 1.60	0.020	ADP-ribosylation factor-like GTPase 10
DOK1	− 1.60	0.025	Docking protein 1
GBP1	− 1.62	0.026	Guanylate-binding protein 1, interferon inducible
PRRX2	− 1.62	0.027	Paired-related homeobox 2
MFI2	− 1.62	0.013	Antigen p97 (melanoma associated) identified by monoclonal antibody
LRRC32	− 1.66	0.046	Leucine-rich repeat-containing 32
IFITM1	− 1.68	0.049	Interferon-induced transmembrane protein 1
HPSE	− 1.69	0.024	Heparanase
PTBP2	− 1.70	0.024	Polypyrimidine tract-binding protein 2
TRAV20	− 1.70	0.025	T-cell receptor alpha variable 20
MIR503HG	− 1.70	0.039	MIR503 host gene
EHBP1L1	− 1.70	0.033	EH domain-binding protein 1-like 1
MIR4540	− 1.71	0.011	microrna 4540
SLC2A1	− 1.71	0.049	Solute carrier family 2 (facilitated glucose transporter)

of dysfunctional endothelium development. To verify the findings obtained from the microarray analysis, we performed real-time PCR analysis to evaluate the upregulated expression of five genes (*ITGB8, CCND2, STAT1, ALDH2*, and *ADAMTS5*). These five genes were selected based on fold change > 1.50 and *p* value < 0.05. Using the IPA software, we focused on investigating the roles of these genes in the inflammatory response, cell movement, cell signaling, and cardiovascular system function and development (Supplementary Table 2, Online Resource 1), which are likely to be involved in the development of a dysfunctional endothelium. PCR results were consistent with the observed changes in gene expression profiles identified in the microarray experiments (Supplementary Table 1, Online Resource 1).

Cyclin D2 binds to the cyclin-dependent kinase, which is essential for entry of cells into the G1 and S phases [29]. Interestingly, *cyclin D2* expression was found to be upregulated in T2D-HUVECs relative to control cells, which could

explain the dramatic increase in the number of cells in the S phase. Consistent with the findings of whole-genome microarray study, *cyclin D2* was upregulated in HUVECs derived from GDM patients [30]. Results of the present study indicated that epigenetic changes induced by hyperglycemia could be responsible for the observed persistent changes in gene expression. However, one study showed that *cyclin D2* overexpression in mice enhanced beta cell proliferation through Akt signaling, which was inconsistent with our currently proposed model, which showed reduced cell proliferation and *cyclin D2* upregulation [31]. Further studies are required to explain why *cyclin D2* overexpression did not promote cell proliferation. Moreover, our results were consistent with an early study demonstrating that *cyclin D2* overexpression did not influence cell growth or viability but altered the cell cycle distribution, as evidenced by the greater proportion of cells in the S phase and reduced proportion of cells in the G0/G1 phase in a

Fig. 4 Clustered display of microarray data and validation of selected genes by real-time PCR. **a** Hierarchical cluster analysis of differentially expressed genes in T2D-HUVEC (group F) compared to C.HUVEC (group N) using data from microarray analysis. Red color shows upregulation, purple color shows no changes and blue color shows downregulation. **b** Validation of microarray results of selected genes in T2D-HUVEC (black bar) compared to C.HUVEC (white bar) using real-time PCR. Gene expression was normalized to β-actin mRNA level in each sample. Data of C-HUVEC at 5 mM have been "normalized" to 1. Results expressed as mean ± SEM of three different donors ($n = 3$). ***$p < 0.0001$, *$p < 0.05$ versus controls
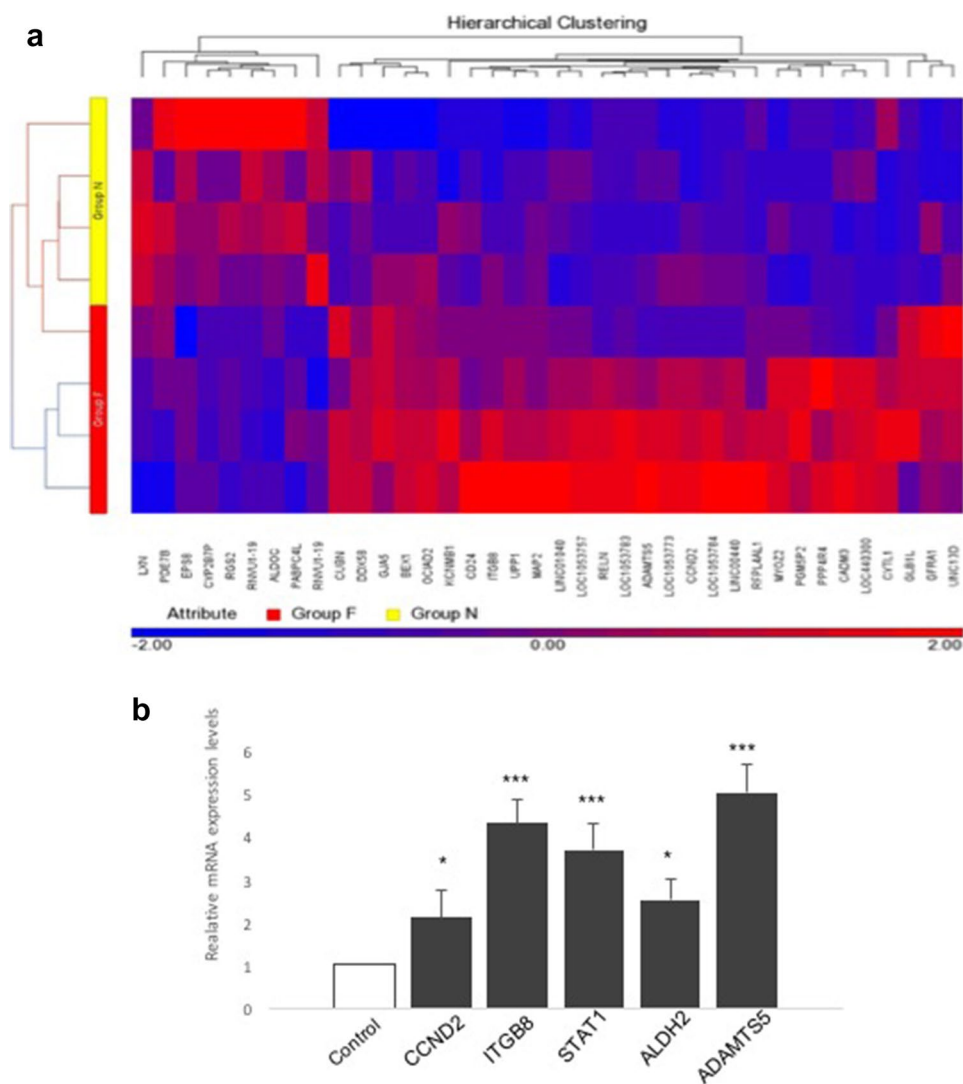
cyclin D2-expressing IL-3-dependent cell line [32]. We suggested that the significant increase in the number of cells in the S phase was caused by a shortened G0/G1 phase and prolonged S phase. Thus, cell growth inhibition in T2D-HUVECs could be mediated by different mechanisms of cell cycle arrest or cell growth. Further studies are required to analyze other proteins involved in cell cycle regulation, such as cyclin D1 and p21.

Increased metabolic stress leads to the activation of STAT1-associated transcription factors [33]. STAT1 is known as a pro-inflammatory and a pro-atherogenic factor via the IFN-gamma and TLR cytokine signaling, which is involved in endothelial dysfunction and cardiovascular diseases [34]. Interestingly, STAT1 regulates cytokine-induced apoptosis through elevation of the pro-apoptotic protein DP5 in pancreatic beta cells [33]. Thus, the observed *STAT1* upregulation could be responsible for increased cell death in T2D-HUVECs. However, further studies are required to verify the above findings.

Integrins are cell adhesion molecules which play a key role in leukocyte homing and cell differentiation in inflammation and cancer [35]. *ITGB8* showed threefold upregulation in T2D-HUVECs relative to controls and was identified by network analysis to be associated with inflammatory response and cardiovascular system function and development (Supplementary Table 2, Online Resource 1). The above findings are consistent with our previous microarray results that showed *ITGB8* upregulation in HUVECs derived from GDM patients relative to C.HUVECs [4], thereby suggesting that *ITGB8* is involved in the pathogenesis of diabetes-induced endothelial dysfunction and associated vascular diseases. Interestingly, a previous in vitro study in endothelial progenitor cells exposed to high glucose (20 mM) showed overexpression of integrins, which altered molecular interactions with the basement membrane and established firmer cell–matrix adhesion interactions [36]. These led to defects in cell migration and proliferation, which is important for the

re-endothelialization process and leads to EC dysfunction and diabetic microvascular complications.

ALDH2 has recently received research attention because of its anti-oxidative properties [37, 38]. The observed *ALDH2* upregulation in T2D-HUVECs could be triggered in response to oxidative stress. *ALDH2* overexpression has been shown to exert protective effects against hyperglycemic stress in coronary ECs derived from type 1 diabetic mice [39]. *ALDH2* downregulation and reduced *ALDH2* activity could potentially contribute to endothelial dysfunction in diabetic cardiomyopathy.

ADAMTS are zinc metalloproteases (MMPs) comprising 20 members, namely, from ADAMTS-1 to ADAMTS-20 [40]. The structures of ADAMTS are related to those of the ADAM and matrix MMP family of proteinases and are primarily present in the extracellular matrix (ECM). In the present study, *ADAMTS5* was found to be upregulated in T2D-HUVECs relative to controls. These findings are consistent with those of a study showing that high glucose levels lead to the *ADAMTS5* upregulation in a human primary glioblastoma cell line [41]. Therefore, we hypothesized that elevated glucose levels play a key role in the synthesis of ADAMTS through unidentified mechanisms.

In addition, in our experiments, we cultured the fetal HUVECs isolated from both type 2 diabetic patients and healthy subjects under normal glucose concentration (5 mM) with no treatment over several passages and our results show that these cells are still damaged even after glucose normalization. This raises the question of the whether the medications were taken by T2D pregnant women such as insulin and others are capable to prevent the fetal endothelial dysfunction worth of further investigation. While we did not directly test the effect of these medications on our model, it has been previously published that the insulin restores the damaging effect of gestational diabetes on HUVEC [42].

The main limitation of this study is the low number of study subjects; however, the values of the statistical significance acquired strongly confirm the validity of the findings. In addition, there were no significant differences in subjects' parameters except higher random glucose levels and HbA1c of the diabetic patients compared to controls. Thus, the observed changes in gene expression could be partially attributed to in utero exposure to hyperglycemia.

Conclusion

Taken together, the persistent changes in gene expression patterns and dysfunctional characteristics associated with T2D include mitochondrial oxidative stress, reduced cell proliferation, altered cell cycle distribution, and increased apoptosis rates in HUVECs derived from T2D mothers. This study highlights the pathological role of maternal T2D on fetal endothelial dysfunction. The data of the current study might help in designing therapeutic drugs which have the capability to reverse changes in fetal endothelial dysfunction induced by maternal type 2 diabetes.

Compliance with ethical standards

Conflict of interest Author declared that they have no conflicts of interest.

Ethical approval All procedures performed in studies involving human participants were in accordance with the ethical standards of the institutional and/or national research committee and with the 1964 Helsinki declaration and its later amendments or comparable ethical standards. Approval of the study was given by the Ethics Committee of the King Abdulaziz University Hospital, Jeddah, Saudi Arabia.

Informed consent Informed consent was obtained from all individual participants included in the study.

References

1. Vanhoutte PM (2010) Regeneration of the endothelium in vascular injury. Cardiovasc Drugs Ther 24(4):299–303. https://doi.org/10.1007/s10557-010-6257-5

2. McLaughlin K, Audette MC, Parker JD, Kingdom JC (2018) Mechanisms and clinical significance of endothelial dysfunction in high-risk pregnancies. Can J Cardiol 34(4):371–380. https://doi.org/10.1016/j.cjca.2018.01.006

3. Zhao Z (2016) Reevaluation of antioxidative strategies for birth defect prevention in diabetic pregnancies. J Biomol Res Ther. https://doi.org/10.4172/2167-7956.1000145

4. Sultan SA, Liu W, Peng Y, Roberts W, Whitelaw D, Graham AM (2015) The role of maternal gestational diabetes in inducing fetal endothelial dysfunction. J Cell Physiol 230(11):2695–2705. https://doi.org/10.1002/jcp.24993

5. Petrie JR, Guzik TJ, Touyz RM (2017) Diabetes, hypertension, and cardiovascular disease: clinical insights and vascular mechanisms. Can J Cardiol. https://doi.org/10.1016/j.cjca.2017.12.005

6. Kvietys PR, Granger DN (2012) Role of reactive oxygen and nitrogen species in the vascular responses to inflammation. Free Radic Biol Med 52(3):556–592. https://doi.org/10.1016/j.freeradbiomed.2011.11.002

7. Biri A, Onan A, Devrim E, Babacan F, Kavutcu M, Durak I (2006) Oxidant status in maternal and cord plasma and placental tissue in gestational diabetes. Placenta 27(2–3):327–332. https://doi.org/10.1016/j.placenta.2005.01.002

8. Senthil KKJ, Gokila VM, Wang SY (2017) Activation of Nrf2-mediated anti-oxidant genes by antrodin C prevents hyperglycemia-induced senescence and apoptosis in human endothelial cells. Oncotarget 8(57):96568–96587. https://doi.org/10.18632/oncotarget.19951

9. Jain M, LoGerfo FW, Guthrie P, Pradhan L (2011) Effect of hyperglycemia and neuropeptides on interleukin-8 expression and angiogenesis in dermal microvascular endothelial cells. J Vasc Surg 53(6):1654–1660. e1652

10. Zhu ZX, Cai WH, Wang T, Ye HB, Zhu YT, Chi LS, Duan YM, Sun CC, Xuan YH, Jin LT (2015) bFGF-regulating MAPKs are involved in high glucose-mediated ROS production and delay of vascular endothelial cell migration. PLoS One 10(12):e0144495. https://doi.org/10.1371/journal.pone.0144495

11. Barker DJ (1998) In utero programming of chronic disease. Clin Sci (Lond) 95(2):115–128. https://doi.org/10.1042/cs0950115

12. Franks PW, Looker HC, Kobes S, Touger L, Tataranni PA, Hanson RL, Knowler WC (2006) Gestational glucose tolerance and risk of type 2 diabetes in young Pima Indian offspring. Diabetes 55(2):460–465. https://doi.org/10.2337/diabetes.55.02.06.db05-0823

13. Dabelea D, Knowler WC, Pettitt DJ (2000) Effect of diabetes in pregnancy on offspring: follow-up research in the Pima Indians. J Matern Fetal Med 9 (1):83–88. https://doi.org/10.1002/(SICI)1520-6661(200001/02)9:1%3C83::AID-MFM17%3E3.0.CO;2-O

14. Handelsman Y, Mechanick JI, Blonde L, Grunberger G, Bloomgarden ZT, Bray GA, Dagogo-Jack S, Davidson JA, Einhorn D, Ganda O, Garber AJ, Hirsch IB, Horton ES, Ismail-Beigi F, Jellinger PS, Jones KL, Jovanovic L, Lebovitz H, Levy P, Moghissi ES, Orzeck EA, Vinik AI, Wyne KL, Plan ATFfDaDCC (2011) American Association of Clinical Endocrinologists Medical Guidelines for clinical practice for developing a diabetes mellitus comprehensive care plan: executive summary. Endocr Pract 17(2):287–302. https://doi.org/10.4158/EP.17.2.287

15. Eccles KA, Sowden H, Porter KE, Parkin SM, Homer-Vanniasinkam S, Graham AM (2008) Simvastatin alters human endothelial cell adhesion molecule expression and inhibits leukocyte adhesion under flow. Atherosclerosis 200(1):69–79. https://doi.org/10.1016/j.atherosclerosis.2007.12.018

16. Quintana-Cabrera R, Fernandez-Fernandez S, Bobo-Jimenez V, Escobar J, Sastre J, Almeida A, Bolanos JP (2012) gamma-Glutamylcysteine detoxifies reactive oxygen species by acting as glutathione peroxidase-1 cofactor. Nat Commun 3:718. https://doi.org/10.1038/ncomms1722

17. hua Yu J, yu Liu C, bin Zheng G, Zhang LY, hui Yan M, yan Zhang W, ying Meng X, fang Yu X (2013) Pseudolaric acid B induced cell cycle arrest, autophagy and senescence in murine fibrosarcoma l929 cell. Int J Med Sci 10(6):707

18. Pfaffl MW (2002) Relative expression software tool (REST(C)) for group-wise comparison and statistical analysis of relative expression results in real-time PCR. Nucleic Acids Res 30(9):36e–36. https://doi.org/10.1093/nar/30.9.e36

19. Alonso-Calvo R, Maojo V, Billhardt H, Martín-Sánchez F, García-Remesal M, Pérez-Rey D (2007) An agent-and ontology-based system for integrating public gene, protein, and disease databases. J Biomed Inform 40(1):17–29

20. Shrestha B, Prasai PK, Kaskas AM, Khanna A, Letchuman V, Letchuman S, Alexander JS, Orr AW, Woolard MD, Pattillo CB (2018) Differential arterial and venous endothelial redox responses to oxidative stress. Microcirculation 20:e12486

21. Patel H, Chen J, Das KC, Kavdia M (2013) Hyperglycemia induces differential change in oxidative stress at gene expression and functional levels in HUVEC and HMVEC. Cardiovasc Diabetol 12(1):142. https://doi.org/10.1186/1475-2840-12-142

22. Villeneuve LM, Natarajan R (2010) The role of epigenetics in the pathology of diabetic complications. Am J Physiol Renal Physiol 299(1):F14–F25. https://doi.org/10.1152/ajprenal.00200.2010

23. Sank A, Wei D, Reid J, Ertl D, Nimni M, Weaver F, Yellin A, Tuan TL (1994) Human endothelial cells are defective in diabetic vascular disease. J Surg Res 57(6):647–653. https://doi.org/10.1006/jsre.1994.1195

24. Wang Q, Yang M, Xu H, Yu J (2014) Tetrahydrobiopterin improves endothelial function in cardiovascular disease: a systematic review. Evid Based Complement Altern Med 2014:850312. https://doi.org/10.1155/2014/850312

25. Su D, Zhou Y, Hu S, Guan L, Shi C, Wang Q, Chen Y, Lu C, Li Q, Ma X (2017) Role of GAB1/PI3K/AKT signaling high glucose-induced cardiomyocyte apoptosis. Biomed Pharmacother 93:1197–1204

26. Boeynaems S, Tompa P, Van Den Bosch L (2018) Phasing in on the cell cycle. Cell Div 13(1):1. https://doi.org/10.1186/s13008-018-0034-4

27. Dimauro I, Sgura A, Pittaluga M, Magi F, Fantini C, Mancinelli R, Sgadari A, Fulle S, Caporossi D (2017) Regular exercise participation improves genomic stability in diabetic patients: an exploratory study to analyse telomere length and DNA damage. Sci Rep 7(1):4137. https://doi.org/10.1038/s41598-017-04448-4

28. Lorenzi M, Cagliero E, Toledo S (1985) Glucose toxicity for human endothelial cells in culture. Delayed replication, disturbed cell cycle, and accelerated death. Diabetes 34(7):621–627. https://doi.org/10.2337/diab.34.7.621

29. Wafa K, MacLean J, Zhang F, Pasumarthi KB (2013) Characterization of growth suppressive functions of a splice variant of cyclin D2. PLoS One 8(1):e53503

30. Ambra R, Manca S, Palumbo MC, Leoni G, Natarelli L, De Marco A, Consoli A, Pandolfi A, Virgili F (2014) Transcriptome analysis of human primary endothelial cells (HUVEC) from umbilical cords of gestational diabetic mothers reveals candidate sites for an epigenetic modulation of specific gene expression. Genomics 103(5–6):337–348. https://doi.org/10.1016/j.ygeno.2014.03.003

31. Stamateris RE, Sharma RB, Kong Y, Ebrahimpour P, Panday D, Ranganath P, Zou B, Levitt H, Parambil NA, O'Donnell CP (2016) Glucose induces mouse beta cell proliferation via IRS2, mTOR and cyclin D2 but not the insulin receptor. Diabetes 5:db150529

32. Ando K, Ajchenbaum-Cymbalista F, Griffin JD (1993) Regulation of G1/S transition by cyclins D2 and D3 in hematopoietic cells. Proc Natl Acad Sci USA 90(20):9571–9575. https://doi.org/10.1073/pnas.90.20.9571

33. Moore F, Naamane N, Colli ML, Bouckenooghe T, Ortis F, Gurzov EN, Igoillo-Esteve M, Mathieu C, Bontempi G, Thykjaer T, Orntoft TF, Eizirik DL (2011) STAT1 is a master regulator of pancreatic {beta}-cell apoptosis and islet inflammation. J Biol Chem 286(2):929–941. https://doi.org/10.1074/jbc.M110.162131

34. Sikorski K, Czerwoniec A, Bujnicki JM, Wesoly J, Bluyssen HA (2011) STAT1 as a novel therapeutical target in pro-atherogenic signal integration of IFNgamma, TLR4 and IL-6 in vascular disease. Cytokine Growth Factor Rev 22(4):211–219. https://doi.org/10.1016/j.cytogfr.2011.06.003

35. Vicente-Manzanares M, Sánchez-Madrid F (2018) Targeting the integrin interactome in human disease. Curr Opin Cell Biol 55:17–23

36. Abplanalp WT, Conklin DJ, Cantor JM, Ginsberg MH, Wysoczynski M, Bhatnagar A, O'Toole TE (2016) Enhanced integrin α4β1-mediated adhesion contributes to a mobilization defect of endothelial progenitor cells in diabetes. Diabetes 5:db160634

37. Guo JM, Liu AJ, Zang P, Dong WZ, Ying L, Wang W, Xu P, Song XR, Cai J, Zhang SQ, Duan JL, Mehta JL, Su DF (2013) ALDH2 protects against stroke by clearing 4-HNE. Cell Res 23(7):915–930. https://doi.org/10.1038/cr.2013.69

38. Zhang Q, Zheng J, Qiu J, Wu X, Xu Y, Shen W, Sun M (2017) ALDH2 restores exhaustive exercise-induced mitochondrial dysfunction in skeletal muscle. Biochem Biophys Res Commun 485(4):753–760

39. Pan G, Deshpande M, Palaniyandi SS (2017) Decreased aldehyde dehydrogenase (ALDH)2 activity contributes to coronary endothelial dysfunction in diabetic cardiomyopathy. J Mol Cell Cardiol 112:135–136. https://doi.org/10.1016/j.yjmcc.2017.07.019

40. Takahashi H, Yuge K, Matsubara S, Ohkuchi A, Kuwata T, Usui R, Suzuki M, Takizawa T (2014) Differential expression of ADAM (a disintegrin and metalloproteinase) genes between human first trimester villous and extravillous trophoblast cells. J Nippon Med Sch 81(3):122–129

41. Akyol S, Ugurcu V, Cakmak O, Altuntas A, Yukselten Y, Akyol O, Sunguroglu A, Demircan K (2016) Evidence for the control of aggrecanases by insulin and glucose in Alzheimer's Disease. Bull Clin Psychopharmacol 24(4):323–332. https://doi.org/10.5455/bcp.20140905124459

42. Salomon C, Westermeier F, Puebla C, Arroyo P, Guzman-Gutierrez E, Pardo F, Leiva A, Casanello P, Sobrevia L (2012) Gestational diabetes reduces adenosine transport in human placental microvascular endothelium, an effect reversed by insulin. PLoS One 7(7):e40578